Nuclear Inst. and Methods in Physics Research, A 892 (2018) 93–97

Contents lists available at ScienceDirect

Nuclear Inst. and Methods in Physics Research, A

journal homepage: www.elsevier.com/locate/nima

Characterization of reticulated vitreous carbon foam using a frisch-grid parallel-plate ionization chamber

Nathaniel S. Edwards [a,*], Jerrod C. Conley [b], Michael A. Reichenberger [a], Kyle A. Nelson [a], Christopher N. Tiner [a], Niklas J. Hinson [a], Philip B. Ugorowski [a], Ryan G. Fronk [a], Douglas S. McGregor [a]

[a] S.M.A.R.T. Laboratory, Department of Mechanical and Nuclear Engineering, Kansas State University, Manhattan, KS 66506, USA
[b] Department of Mechanical and Nuclear Engineering, Kansas State University, Manhattan, KS 66506, USA

ARTICLE INFO

Keywords:
RVC foam
Charge carrier propagation
Frisch grid
Parallel-plate ionization chamber
Gas-filled radiation detector

ABSTRACT

The propagation of electrons through several linear pore densities of reticulated vitreous carbon (RVC) foam was studied using a Frisch-grid parallel-plate ionization chamber pressurized to 1 psig of P-10 proportional gas. The operating voltages of the electrodes contained within the Frisch-grid parallel-plate ionization chamber were defined by measuring counting curves using a collimated ^{241}Am alpha-particle source with and without a Frisch grid. RVC foam samples with linear pore densities of 5, 10, 20, 30, 45, 80, and 100 pores per linear inch were separately positioned between the cathode and anode. Pulse-height spectra and count rates from a collimated ^{241}Am alpha-particle source positioned between the cathode and each RVC foam sample were measured and compared to a measurement without an RVC foam sample. The Frisch grid was positioned in between the RVC foam sample and the anode. The measured pulse-height spectra were indiscernible from background and resulted in negligible net count rates for all RVC foam samples. The Frisch grid parallel-plate ionization chamber measurement results indicate that electrons do not traverse the bulk of RVC foam and consequently do not produce a pulse.

1. Introduction

Recently, foam structures, particularly reticulated vitreous carbon (RVC) foam, have emerged as thin-film-coated substrates for neutron detection applications [1–8]. RVC foam, produced by ERG Aerospace Corporation, is composed of a semi-randomized network of struts, cells, and pores, in which the cells and pores within the bulk of the material are defined by the vacancies between neighboring struts [9] as shown in Fig. 1. The size and number of struts, cells, and pores contained within the RVC foam defines the linear pore density of the material and RVC foams are available with linear pore densities ranging from 5–100 pores per linear inch (PPI). Pore diameters can range in size from 4.85 ± 0.81 mm to 0.63 ± 0.12 mm for linear pore densities of 5 to 80 PPI RVC foam samples [8], respectively, indicating an inverse relation between linear pore density and average pore diameter. RVC foams are also suitable for use in high-temperature environments, such as those experienced in oil-well logging where instruments have required operational and survival temperatures ranging up to 175 °C and 200 °C, respectively [10,11], because the material has temperature limitations up to 315 °C and 3499 °C in air and inert environment, respectively [12]. Currently, RVC foams are used for a variety of applications such as energy absorbers, heat shielding, and fuel cells [13], and therefore the manufacturing infrastructure is already in place.

The propagation of electrons through the bulk of RVC foam was previously studied using a parallel-plate ionization chamber in order to determine whether RVC foam could be used as a coating substrate with the potential to possess high intrinsic thermal neutron detection efficiency capabilities [7]. Although measured count rates and pulse-height spectra provided some insight into the propagation of electrons through the bulk of RVC foam, further characterization efforts were necessary to improve the confidence of the observations. The implementation of a Frisch grid between a RVC foam sample and a planar anode should further clarify whether electrons are capable of traversing the bulk of the RVC foam sample since the measured pulse-height spectra and count rates are representative of charge induction specifically between the Frisch grid and the anode [14,15]. Thus, the present work conveys the examination of the propagation of electrons through the bulk of RVC

* Corresponding author.
E-mail address: nedwards@ksu.edu (N.S. Edwards).

https://doi.org/10.1016/j.nima.2018.03.005
Received 8 November 2017; Received in revised form 24 February 2018; Accepted 2 March 2018
Available online 9 March 2018

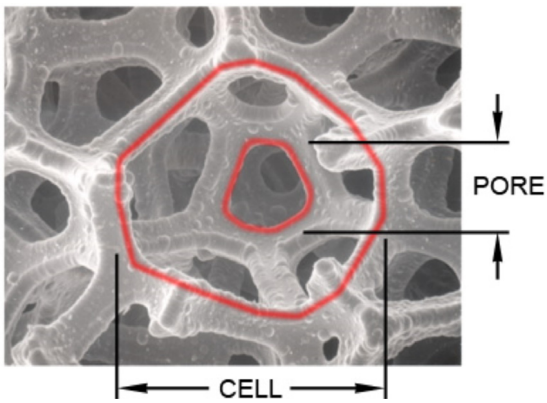

Fig. 1. Structural definition of RVC foam indicating the pores and cells formed by neighboring struts [9].

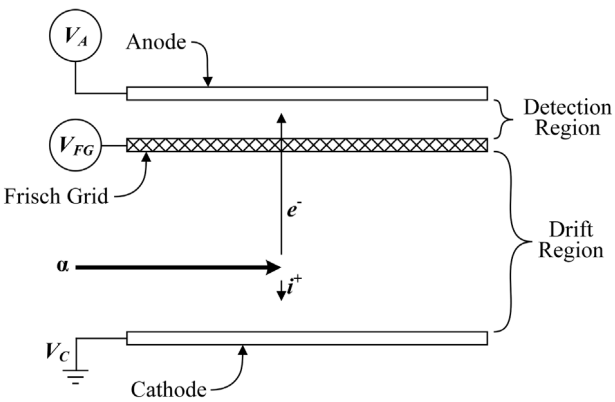

Fig. 2. Operation of a parallel-plate ionization chamber with a Frisch grid between the anode and cathode. Formation of a measurable signal on the anode only occurs for charges moving within the detection region. The operating voltage of the anode, V_A, is set higher than that of the Frisch grid, V_{FG}, which is set above the operating voltage of the cathode, V_C (typically maintained at ground potential).

foam samples, with linear pore densities ranging between 5 and 100 PPI, using a Frisch-grid parallel-plate ionization chamber.

2. Theoretical considerations

The application of a grid to a gas-filled parallel-plate ionization chamber was introduced in 1942 by Otto Frisch as a means of improving the uniformity of the chamber sensitivity to incident radiation quanta [14]. The implementation of a Frisch grid between planar anode and cathode electrodes allows the device to measure induced charge only between the Frisch grid and anode. Fig. 2 illustrates a typical parallel-plate ionization chamber with a Frisch grid implemented. As radiation quanta, such as alpha particles, cause ionization within the drift region, electrons and positively-charged ions travel toward the Frisch grid and cathode, respectively, due to the electric field formed from the potential difference between the Frisch grid and cathode. The operating voltages of the Frisch grid and cathode, V_{FG} and V_C, respectively, require that $V_{FG} > V_C$ in order to drift electrons toward the Frisch grid and positively-charged ions toward the cathode (the cathode is commonly maintained at ground potential). Once electrons pass through the Frisch grid, charge is induced on the anode as electrons drift through the detection region influenced by the electric field between the Frisch grid and anode, with the required operating voltage condition of $V_A > V_{FG}$.

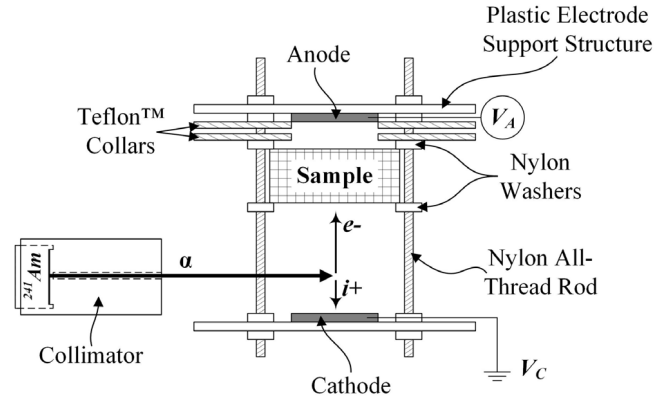

Fig. 3. Test configuration used for measuring the propagation of electrons through RVC foam. Electrons and positively-charged ions are created due to ionization from alpha particles injected below the sample location and the electric field formed between the anode and cathode causes the electrons and ions to drift toward their respectively-charged electrodes.

3. Experimental procedure

The propagation of electrons through the bulk of RVC foam was studied using a parallel-plate ionization chamber without and with a Frisch grid, as shown in Figs. 3 and 4, respectively. The planar electrodes, each 12.7-mm diameter, were fabricated using 3.18-mm (0.125-in.) thick aluminum and were specifically designed to ensure that the resulting electric field would only penetrate through the bulk of the 6.35-mm (0.25-in.) thick RVC samples. A distance of approximately 29 mm was maintained between the planar electrodes and the Frisch grid was positioned between the electrodes, approximately 0.79-mm below the surface of the anode. The custom-designed, 25.4-μm thick BeCu Frisch-grid electrode shown in Fig. 5 was fabricated by Tech-Etch, Inc. [16] and contained 25.4-μm wide strips of metal with vertical and horizontal pitches of approximately 1.6 mm. Teflon™ collars were positioned around the Frisch grid, as shown in Fig. 4, to ensure that electrons were streaming through, rather than around, the bulk of the RVC sample. The Teflon™ collars measured 0.79-mm thick with internal and external diameters of approximately 12.7 mm and 50.8 mm, respectively. Furthermore, the application of the Teflon™ collars above and below the Frisch grid negated the need to surround the entire RVC sample with a Teflon™ collar, as was previously implemented [7], and reduced the probability of obstructing the incident beam of alpha particles. A collimated-^{241}Am alpha-particle source was positioned approximately 10-mm above the cathode in such a way to allow for the 5.48-MeV alpha particles to deposit a majority of their energy within the electric field between the electrodes as defined by the characteristic Bragg curve [17]. The collimator contained a 2-mm diameter aperture with a collimation length of 10 mm, resulting in a beam of alpha particles with a chord length of 15.6 mm at the extent of the range of the emitted alpha particles (43.9 mm) in 1 psig of P-10 proportional gas (90% argon and 10% methane) [17]. The testing apparatus and collimated ^{241}Am alpha-particle source were contained within a sealed aluminum enclosure backfilled with P-10 gas at a constant pressure of 1 psig throughout the duration of each measurement.

The parallel-plate electrode configuration without the Frisch grid was characterized via a counting curve to verify the expected operating voltage required to attain an electron saturation velocity of approximately 0.3 V cm^{-1} Torr^{-1} in 1 psig of P-10 [15,18]. The distance between the planar electrodes was held constant with and without the Frisch grid to maintain the resulting electric field strength. The resulting anode operating voltage, V_A, was set to 700 V to achieve a sufficient drift electric field strength between the planar electrodes, with the cathode operating voltage, V_C, maintained at ground potential. Next, the Frisch

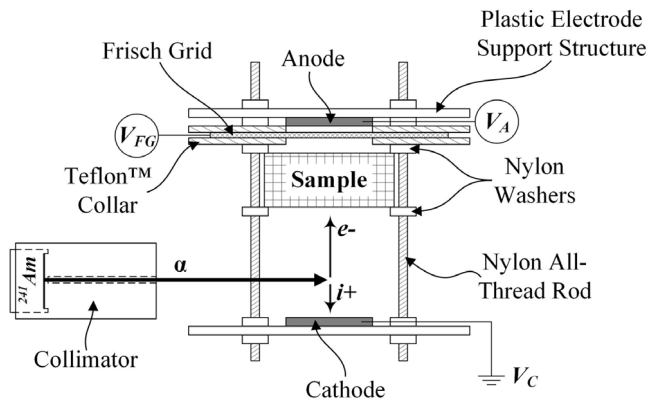

Fig. 4. Modified test configuration to measure the propagation of electrons through various linear pore densities of RVC foam using a Frisch grid positioned between the sample and the anode. The Frisch-grid operating voltage, V_{FG}, is set below that of the anode, V_A, in order to drift electrons from the Frisch grid to the anode.

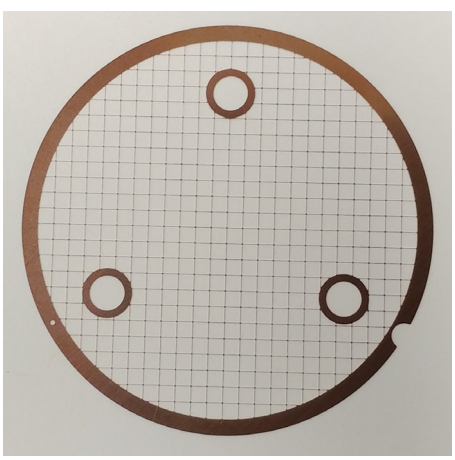

Fig. 5. BeCu Frisch grid fabricated by Tech Etch containing 25.4-μm wide strips of metal with vertical and horizontal pitches of approximately 1.6 mm.

grid was installed between the planar electrodes and a second counting curve was produced in which the Frisch-grid operating voltage, V_{FG}, was maintained at 700 V, the cathode was again maintained at ground potential, and the anode operating voltage was increased in increments of 50 V from 0 to 1650 V. The resulting anode applied voltage was determined to be 1500 V.

With these operating voltage parameters defined, a two-hour measurement was conducted without a RVC sample present to establish a control for the experiment and the measured count rate and pulse-height spectrum were recorded. The control measurement was conducted for the electrode configurations with and without the Frisch grid. Subsequent two-hour measurements were also performed for 6.35-mm (0.25 in.) thick RVC foam samples with linear pore densities of 5, 10, 20, 30, 45, 80, and 100 PPI with and without the Frisch grid installed. In each scenario with a RVC sample installed in between the cathode and Frisch grid, the sample position was maintained at a distance of approximately 17 mm from the cathode surface to ensure that any charge induction occurring from the site of charge injection to the bottom surface of the sample was maintained throughout all trials. The measurements conducted without the Frisch grid served to ensure that the system was functioning similar to previous measurements [7].

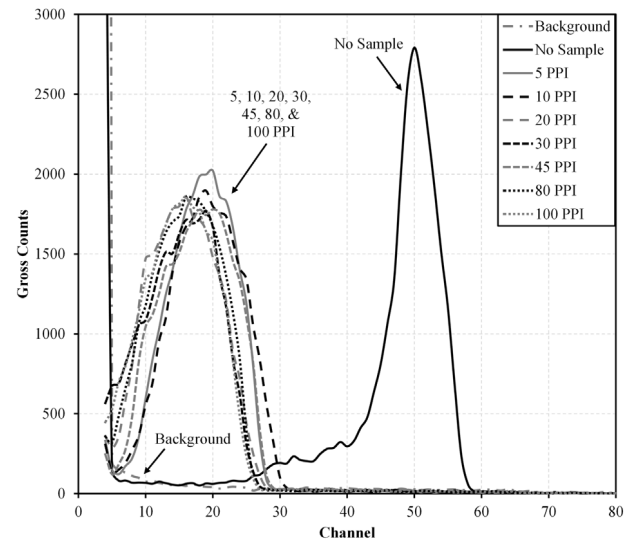

Fig. 6. Pulse-height spectra measured using the testing configuration without the Frisch grid installed. The presence of pulses above background indicates that charge induction occurred. The location of charge induction was suspected to have occurred between the cathode and RVC foam position as well as potentially at shallow depths within the RVC foam sample.

Table 1
Net count rates measured for a collimated ^{241}Am alpha-particle source using the testing configuration shown in Fig. 3. The alpha-particle beam was positioned between the cathode and RVC foam sample locations.

Sample	Net count rate (counts second^{-1})
No Sample	3.47 ± 0.02
5 PPI	3.31 ± 0.03
10 PPI	3.37 ± 0.03
20 PPI	3.00 ± 0.03
30 PPI	2.74 ± 0.03
45 PPI	3.25 ± 0.03
80 PPI	3.04 ± 0.03
100 PPI	2.89 ± 0.03

4. Results and discussion

Shown in Fig. 6 are the pulse-height spectra measured without the Frisch grid installed for the various RVC foam linear pore densities compared to the no sample case. The measured net count rates are listed in Table 1. These results are similar to those previously measured [7] and suggest that charge induction occurred for each measurement. Given the down-shift in peak-channel number of the pulse-height spectra measured with the RVC foam samples relative to the no sample case, it was previously suspected that these results indicate that charge induction was occurring between the sample and the cathode and potentially at shallow depths within the sample.

Shown in Fig. 7 are the measured pulse-height spectra with the Frisch grid installed for the various RVC foam linear pore densities compared to the no sample case. Negligible net count rates were measured for each of the RVC foam samples due to the blending of the measured pulse-height spectra with the background signal. The substantial reduction in pulse amplitude, compared to the case with no sample, indicates that minimal, if any, charge induction occurred between the Frisch grid and anode for all RVC linear pore densities tested. Therefore, given the measured pulse-height spectra and negligible net count rates for charge induction occurring between the Frisch grid and anode, electrons do not traverse the bulk of RVC foam with linear pore densities ranging from 5–100 PPI.

The lack of capability for electrons to drift out of the bulk of RVC foam presents a challenge for these substrates to be considered as a compact substrate capable of possessing an abundance of active

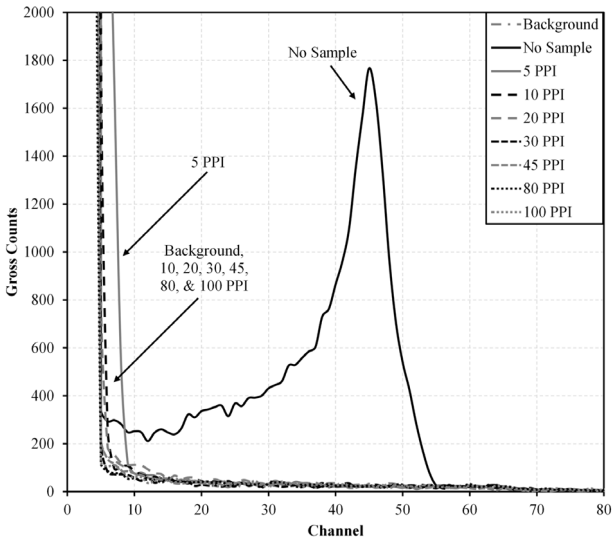

Fig. 7. Measured pulse-height spectra produced from electrons that traversed beyond the Frisch grid for various linear pore densities of RVC foam.

thin-film-coated surfaces. A potential solution would be to use several of the thin-film-coated RVC foam samples with collecting electrodes positioned adjacent to each sample, similar to the orientation of foils and anode wires within lithium-foil multi-wire proportional counters [19]. However, this solution requires several RVC foam samples in order to be capable of achieving the neutron detection performance of commercial ^{3}He proportional counters [15,20].

One alternative solution to overcoming the issue of electrons not being capable of traversing through the bulk of RVC foam is to incorporate so-called "macrostructures", such as channels or cylindrical voids oriented in the direction of the electric field lines, into the bulk of the sample. These macrostructures would allow for charge carriers produced within the bulk of the sample to possess a higher probability of escaping the sample and subsequently inducing charge as they drift toward their respectively-charged electrodes, unimpeded by sample features. Although the incorporation of macrostructures would reduce the overall amount of thin-film-coated surface area within a sample, the quantity of active thin-film-coated surfaces within the sample would increase. A second alternative solution would be to consider other compact substrate types containing an abundance of surface area for applying thin-film coatings. Recently, honeycomb substrates have emerged as thin-film-coated substrates due to the large amount of surface area contained within a compact sample [3,21–27]. The substrate can thus be oriented in such a way that allows charge carriers created within the sample to drift out of the substrate and toward their respectively-charged electrodes.

5. Conclusions

The ability for electrons to traverse the bulk of 6.35-mm thick RVC foam samples with linear pore densities ranging from 5–100 PPI was studied using a parallel-plate ionization chamber with and without a Frisch grid installed between the RVC foam and anode positions. The measured pulse-height spectra and net count rates with the Frisch grid installed indicate that electrons do not traverse the bulk of RVC foam samples with linear pore densities ranging from 5–100 PPI. As a result, RVC foam samples that are used as coating substrates for neutron detection applications will only be sensitive to conversion of measurable reaction products at approximately the exterior surfaces of the RVC foam sample that are exposed to the surrounding backfill gas. Thus, the maximum intrinsic thermal neutron detection efficiency of RVC foam samples are limited to 4%–5% which is common for thin-film-coated devices [20]. Proposed solutions to the limited intrinsic thermal neutron detection efficiency of a thin-film-coated RVC foam sample include (a) using several thin-film-coated RVC foam samples, (b) incorporating macrostructures into the bulk of the neutron absorbing sample, and (c) the consideration of other compact substrate types containing an abundance of surface area for applying thin-film coatings (such as honeycomb structures). These latter two proposed solutions would allow for charge carriers produced within the bulk of the sample to possess a higher probability of being capable of drifting outside of the sample to their respective electrodes.

Acknowledgments

This work was supported in part by the U.S. Defense Threat Reduction Agency (DTRA), under contract HDTRA1-12-c-0002. The Frisch-grid parallel-plate ionization chamber fabrication and characterization as well as the reticulated vitreous carbon foam measurements were conducted at the Kansas State University Semiconductor Materials and Radiological Technologies (S.M.A.R.T.) Laboratory (Manhattan, KS). The Frisch grid electrode was fabricated by Tech-Etch, Inc.

References

[1] K.A. Nelson, S.L. Bellinger, B.W. Montag, J.L. Neihart, T.A. Riedel, A.J. Schmidt, D.S. McGregor, Investigation of aerogel, saturated foam, and foil for thermal neutron detection, in: 2011 IEEE Nuclear Science Symposium and Medical Imaging Conference, NSS/MIC, Valencia, Spain, Oct. 23-29, paper N20-2, pp. 1026–1029.
[2] K.A. Nelson, J.L. Neihart, T.A. Riedel, A.J. Schmidt, D.S. McGregor, A novel method for detecting neutrons using low density high porosity aerogel and saturated foam, Nucl. Instrum. Methods A 686 (2012) 100–105.
[3] K.A. Nelson, An Investigation of Aerogels, Foams, and Foils for Multi-Wire Proportional Counter Neutron Detectors, in: Mechanical and Nuclear Engineering, Kansas State University, 2013.
[4] C.M. Lavelle, R.M. Deacon, D.S. Hussey, M. Coplan, C.W. Clark, Characterization of boron coated vitreous carbon foam for neutron detection, Nucl. Instrum. Methods A 729 (2013) 346–355.
[5] M.A. Reichenberger, R.G. Fronk, J.K. Shultis, S.R. Stevenson, N.S. Edwards, K.A. Nelson, D.S. McGregor, Monte Carlo simulation of energy deposition by neutron reaction products in lithiated foam using dynamic path generation, in: 2014 IEEE Nuclear Science Symposium and Medical Imaging Conference, NSS/MIC, Seattle, WA, Nov. 8–15, 2014, paper N04-8, p. 3.
[6] C.M. Lavelle, M. Coplan, E.C. Miller, A.K. Thompson, A.L. Kowler, R.E. Vest, A.T. Yue, T. Koeth, M. Al-Sheikhly, C.W. Clark, Demonstration of neutron detection utilizing open cell foam and noble gas scintillation, Appl. Phys. Lett. 106 (2015) 094103.
[7] N.S. Edwards, K.A. Nelson, C.N. Tiner, N.J. Hinson, P.B. Ugorowski, R.G. Fronk, M.A. Reichenberger, D.S. McGregor, Charge propagation through- and neutron sensitivity of- reticulated vitreous carbon foam, in: 2015 IEEE Nuclear Science Symposium and Medical Imaging Conference, NSS/MIC, San Diego, CA, Oct. 31–Nov. 7, 2015, paper N5A3-5, p. 4.
[8] M.A. Reichenberger, R.G. Fronk, J.K. Shultis, J.A. Roberts, N.S. Edwards, S.R. Stevenson, C.N. Tiner, D.S. McGregor, Monte Carlo simulation of random, porous (foam) structures for neutron detection, Radiat. Phys. Chem. 130 (2017) 186–195.
[9] ERG Aerospace Corporation, The Basics of Duocel® Foam, available at http://ergaerospace.com/technical-data/the-basics-of-duocel-foam/, February 15.
[10] A. Nikitin, S. Bliven, Needs of well logging industry in new nuclear detectors, in: IEEE Nuclear Science Symposuim & Medical Imaging Conference, Knoxville, TN, Oct. 30–Nov. 6, 2010, pp. 1214–1219.
[11] Standard Geophysical Detectors, available at http://www.crystals.saint-gobain.com/sites/imdf.crystals.com/files/documents/standard-geophysical-detectors_69792.pdf, February 15.
[12] ERG Aerospace Corporation, Duocel® Reticulated Vitreous Carbon (RVC) Foam, available at http://ergaerospace.com/materials/duocel-reticulated-vitreous-carbon-rvc-foam/,February 15.
[13] ERG Aerospace Corporation, Duocel® Foam Properties & Application Guide, available at http://ergaerospace.com/applications/, February 15.
[14] O.R. Frisch, Isotope Analysis of Uranium Samples by means of their alpha-Ray Groups, British Atomic Energy Report, BR-49, 1942.
[15] G.F. Knoll, Radiation Detection and Measurement, fourth ed., John Wiley & Sons, Inc., Hoboken, NJ, 2010.
[16] Tech-Etch, Inc., available at https://www.tech-etch.com/.
[17] J.F. Ziegler, J.P. Biersack, SRIM-2013 code, in: IBM Company, 2013.
[18] F. Sauli, Gaseous Radiation Detectors: Fundamentals and Applications, Cambridge University Press, 2014.

[19] K.A. Nelson, S.L. Bellinger, B.W. Montag, J.L. Neihart, T.A. Riedel, A.J. Schmidt, D.S. McGregor, Investigation of a lithium foil multi-wire proportional counter for potential ^{3}He replacement, Nucl. Instrum. Methods A 669 (2012) 79–84.

[20] D.S. McGregor, M.D. Hammig, Y.H. Yang, H.K. Gersch, R.T. Klann, Design considerations for thin film coated semiconductor thermal neutron detectors—I: basics regarding alpha particle emitting neutron reactive films, Nucl. Instrum. Methods A 500 (2003) 272–308.

[21] D.S. McGregor, S.L. Bellinger, W.J. McNeil, M.F. Ohmes, K.A. Nelson, Gas-filled neutron detectors having improved detection efficiency, US8519350B2, Aug. 27, 2013.

[22] Y. Yang, C. Li, C. Chen, X. Wang, Y. Li, Research of boron lined honey-comb neutron detector realized with atomic layer deposition, in: 2013 IEEE Nuclear Science Symposium and Medical Imaging Conference, 2013 NSS/MIC, Oct. 27–Nov. 2, 2013, paper N7-1, p. 3.

[23] Z. Fang, Y. Yang, Y. Li, The research of high detection efficiency boron lined detector with a honeycomb neutron converter, in: 2015 IEEE Nuclear Science Symposium and Medical Imaging Conference, NSS/MIC, Oct. 31–Nov. 7 2015, paper N5A3-3, p. 4.

[24] Z. Fang, Y. Yang, Y. Li, X. Wang, Working gas selection of the honeycomb converter-based neutron detector, IEEE Trans. Nucl. Sci. 64 (2017) 1683–1688.

[25] Z. Fang, Y. Yang, Y. Li, Z. Zhang, X. Wang, Research on a neutron detector with a boron-lined honeycomb neutron converter, IEEE Trans. Nucl. Sci. 64 (2017) 1048–1055.

[26] N.S. Edwards, K.A. Nelson, N.J. Hinson, C.N. Tiner, M.A. Reichenberger, D.S. McGregor, Neutron sensitivity of $^{10}B_4C$-coated aluminum honeycomb using a single-anode wire, P-10 continuous-gas-flow proportional counter, Nucl. Instrum. Methods A, submitted for publication.

[27] N.S. Edwards, K.A. Nelson, M.A. Reichenberger, R.G. Fronk, D.S. McGregor, Simulation and optimization of $^{10}B_4C$-coated aluminum honeycomb as a neutron conversion material, Nucl. Instrum. Methods A, submitted for publication.